A VISCOUS STARTER SOLUTION FOR SHUTTLE FLOW FIELD COMPUTATIONS

By
C. P. Li
Lockheed Electronics Company, Inc.
Houston Aerospace Systems Division
Houston, Texas

and
W. D. Goodrich
NASA Manned Spacecraft Center
Houston, Texas

SUMMARY

A time-dependent numerical procedure that calculates the viscous flow in the shock layer around the shuttle nose has been developed. It has been applied to the free-stream conditions that may be encountered in the shuttle flight trajectory and found to be efficient and in satisfactory agreement with other steady and unsteady techniques. Two features associated with the present formulation are responsible for its successful applications. The first is that the flow field computation is made within the shock layer; the second is that the mapping of the computational region places proportionately more mesh points in the vicinity of the wall than in the remaining computational region. Qualitative agreement is also obtained with experimental heat transfer and skin friction coefficients for $Re_\infty = 5000$, at which point the thin boundary layer concept is no longer valid. This procedure is presently developed for a 2D geometry; however, it can be readily modified to consider an angle-of-attack case if used

Page intentionally left blank

in conjunction with a larger and faster computer than the UNIVAC 1108 system at the Manned Spacecraft Center (MSC). The numerical results may be used for low-altitude flight to determine the edge conditions for a thin boundary layer, to provide initial boundary layer profiles for downstream boundary layer calculations, and to start supersonic computations. For high-altitude flight, it may be used to determine the complete flow field in the nose region and also provide a starter solution for subsequent supersonic flow computations.

STARTER SOLUTION DEVELOPMENT

(Figure 1)

The NASA Manned Spacecraft Center and Lockheed Electronics Company, Inc., at Houston have been active in computational flow field development for the past 2-1/2 years. This effort has been concentrated on using the time-dependent finite-difference technique to compute flow fields based on the continuum theory. Applications of the numerical technique have included the inviscid, ideal gas and equilibrium and chemical nonequilibrium air in the shock layer around the Apollo command module at an angle of attack and both the inviscid and viscous flow calculations for a shuttle orbiter wing and nose. In the viscous formulation the shock layer and the laminar wake were considered in order to analyze the flow-separation problem. Since the computer code that calculates the complete flow field around a blunt body has not been completed, we will stress the shock layer flow field in this discussion. Note that our development of a viscous starter solution could be used in conjunction with the plan now being executed at the NASA Ames Research Center under the category of inviscid solutions.[1]

STARTER SOLUTION DEVELOPMENT

INVISCID FLOW

2D
- CARTESIAN COORDINATES
- IDEAL GAS
- EQUILIBRIUM AIR
- DISSOCIATING DIATOMIC GAS

3D
- SPHERICAL POLAR COORDINATES
- IDEAL GAS
- EQUILIBRIUM AIR
- DISSOCIATING DIATOMIC GAS
- FINITE-RATE AIR

VISCOUS FLOW

2D
- CARTESIAN COORDINATES
- IDEAL GAS
- EQUILIBRIUM AIR

Figure 1

FLOW FIELD DESCRIPTION

(Figure 2)

The interest in the flow field computation at the leeward side of the shuttle vehicle at a high angle of attack stems predominately from the aerodynamic heating problem associated with the vast surface area in the leeward flow region as well as the L/D prediction problem at high attitude. With the recent advance in numerical techniques, it seems possible to compute the complete flow around the vehicle by a unified scheme. The flow field may be divided into the shock layer and the laminar near wake that can be extended downstream until turbulence begins.

The flow field at a low angle of attack is relatively simple since it is predominately supersonic downstream of a small subsonic nose region. The viscous shock layer calculation has primary applications in three areas. It can be used to properly start the inviscid supersonic solution since the boundary layer displacement is included. It can also be used to initiate a boundary layer calculation adjacent to the body and downstream from the subsonic region. This latter application is required to augment the downstream inviscid solution. A third possible application is the prediction of flow properties for high-altitude flight when rarefaction effects become important.

FLOW FIELD DESCRIPTION

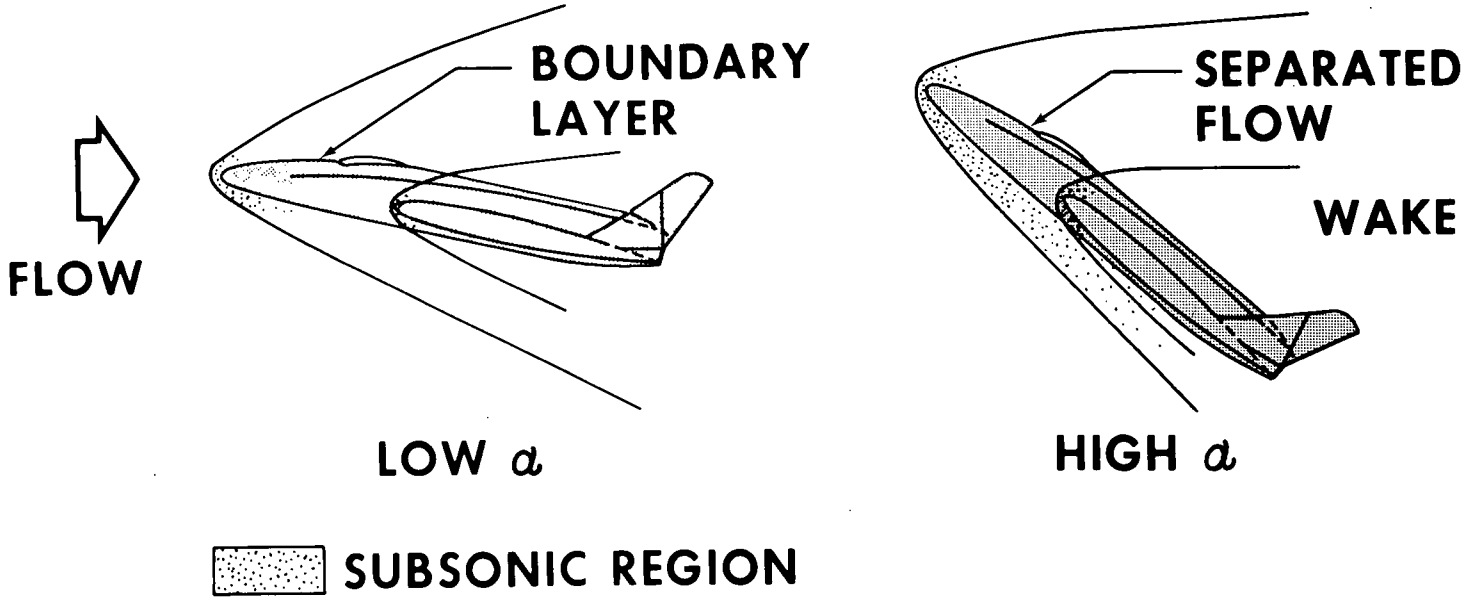

Figure 2

SPACE SHUTTLE TRAJECTORY

(Figure 3)

The importance of analyzing the viscous shock layer can be seen in this figure. It shows the velocity-altitude curves for a typical shuttle trajectory during launch and reentry. Also shown here are boundaries indicating two important flow regions taken from Probstein.[2] These boundaries, however, are relatively arbitrary in nature because of the dependence on the configuration and surface temperature. This figure is therefore intended to indicate the flow dynamics problem that might arise during shuttle flight. The top curve defines the upper boundary in altitude and velocity for which continuum assumption remains valid, while the bottom one denotes the boundary of departure from the classical thin boundary layer concept. It is then seen that all the significant heating and pressure occurs in the boundary layer and viscous layer regimes. The term *viscous layer* refers to the thickening of the boundary layer until the shock layer is fully viscous and the shock wave thickness is about the order of the shock layer.

SPACE SHUTTLE TRAJECTORY
(HIGH HEATING LOAD, LONG CROSS RANGE ORBITER)

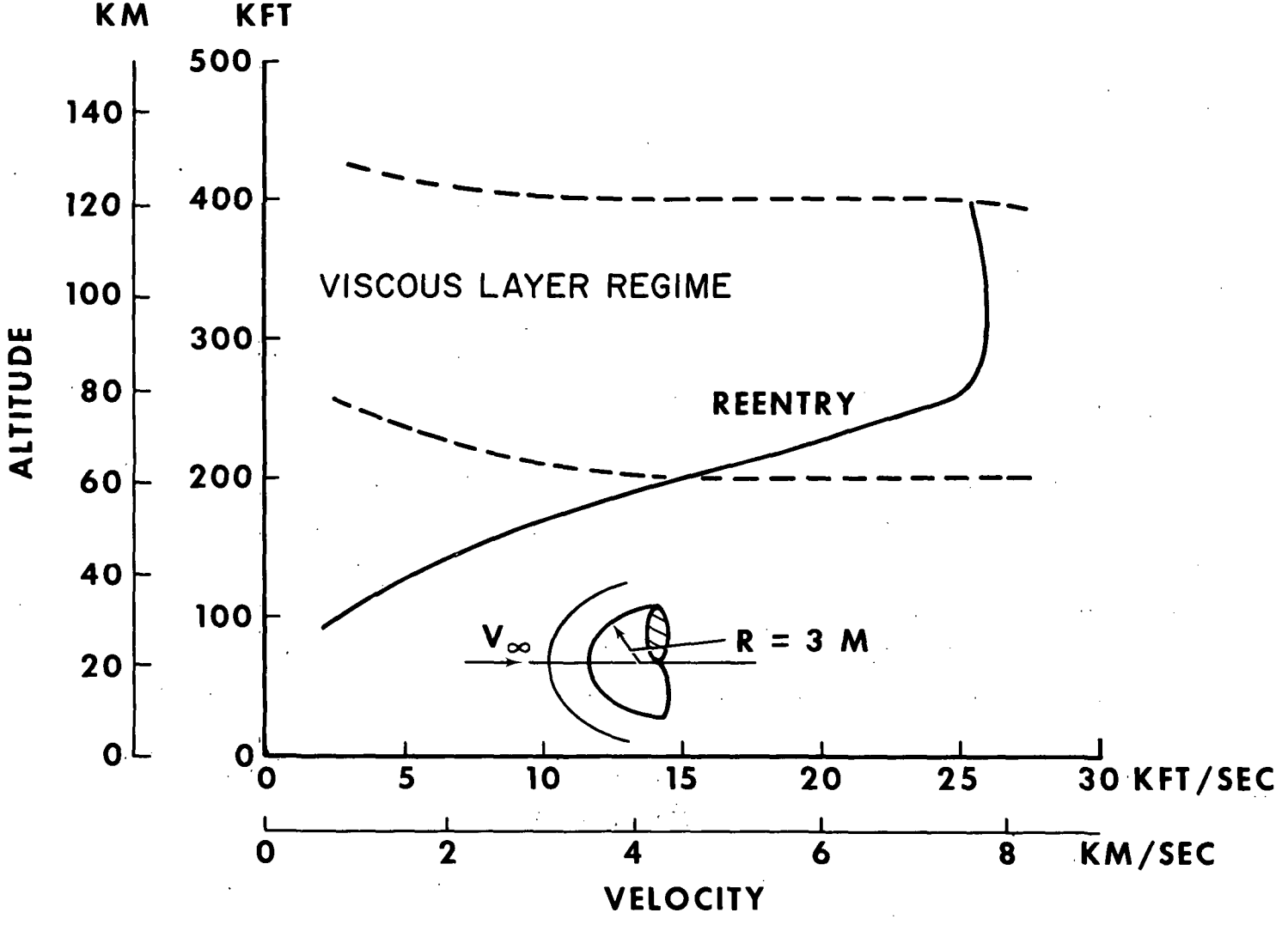

Figure 3

STEADY METHOD

(Figure 4)

This subject has received much attention, and there are many excellent works using various numerical techniques. These formulations are generally valid from low altitudes, where the boundary layer concept is useful, to high altitudes, where they begin to overlap with the kinetic approach. There are at least three methods of solution for the flow along the stagnation streamline: the thin-layer approximation, the higher order boundary layer approximation, and the direct integration through the shock. The first two methods have been applied to the flow downstream of the stagnation point with excellent results. A major assumption used in these two methods is that the shock wave structure does not affect the shock layer solution, or the shock wave is not as thick as the shock layer. The past effort has been reviewed by Cheng.[3]

STEADY METHOD

STAGNATION STREAMLINE

- THIN SHOCK LAYER APPROXIMATION
- HIGHER ORDER BOUNDARY LAYER APPROXIMATION
- DIRECT INTEGRATION THROUGH SHOCK

SHOCK LAYER

- THIN SHOCK LAYER APPROXIMATION
- HIGHER ORDER BOUNDARY LAYER APPROXIMATION

Figure 4

UNSTEADY TECHNIQUE

(Figure 5)

The unsteady or time-dependent technique has been applied in recent years by Scala and Gordon[4] and others to solve the viscous blunt-body problem. This approach has certain advantages over the steady techniques in solving for the flow field not limited to the stagnation point. One is that since the full Navier-Stokes equations are used, the high-order effects on the thin boundary layer are automatically included, and the thin shock layer thickness is not required a priori. In the time-dependent technique a convergent, time-asymptotic solution is obtained if certain stability criteria are met. Most past efforts in solving the unsteady Navier-Stokes equations are similar to the direct integration technique in the steady method, which has been shown to match the free molecular flow limit smoothly at very low Reynolds numbers. Unlike the steady technique that is applicable to the stagnation streamline only, however, these time-dependent techniques are more general and often far more expensive in computing cost because of the nature of the time-marching procedure. To circumvent the prohibitive costs of the large computational domain associated with vehicles at an angle of attack, we decided to follow Moretti's approach[5] in which the flow field within the shock layer was considered. This restricts the technique to flow regimes where the shock wave structure does not influence the shock layer solution.

UNSTEADY TECHNIQUE

- DIRECT PROBLEM
- TWO-LAYER FLOW MODEL
- MODIFIED RANKINE-HUGONIOT RELATIONS
- FINITE-DIFFERENCE MATCHING PROCEDURE FOR SHOCK
- TWO-STEP METHOD IN TIME-MARCHING
- VALID FOR ARBITRARY REYNOLDS NUMBER

Figure 5

BASIC FORMULATION

(Figure 6)

The basic equations of our study are the Navier-Stokes equations plus the nonslip and no-jump conditions for velocity and temperature along the wall. A simple gas model is used to take into account the ideal gas and the equilibrium air properties. In addition, the bulk viscosity is taken to be identically zero, and only plane and axisymmetric flows are considered.

The computational region is enclosed by the inner edge of the shock wave, the body, the axis of symmetry, and the upper boundary. A new set of independent variables is introduced that maps the region into a rectangle with the shock and the body parallel to each other. Further mappings are used to place more mesh points adjacent to the body according to an exponential law. The final mesh consists of uniformly spaced lines in both of the new coordinate axes. The dependent flow variables are chosen as the pressure, the velocity components, and the entropy to suit the Mollier chart for air. More details are given in reference 6.

BASIC FORMULATION

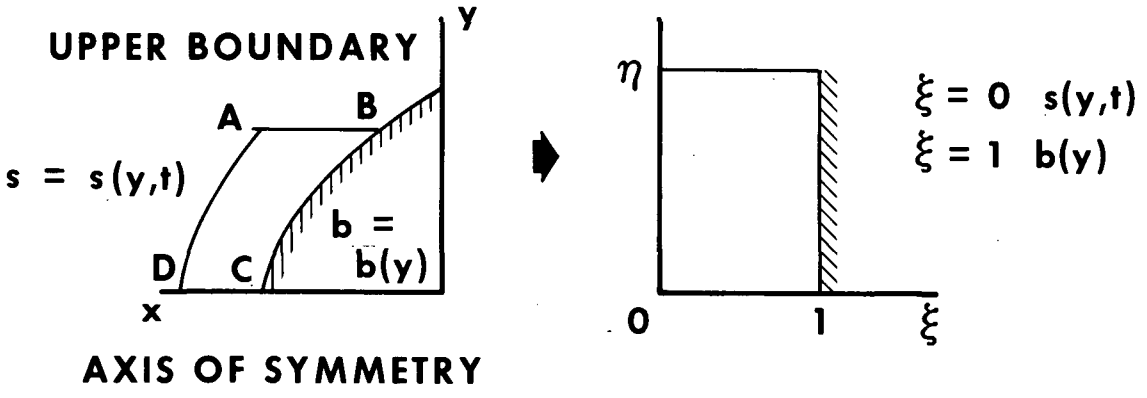

MAPPING 1

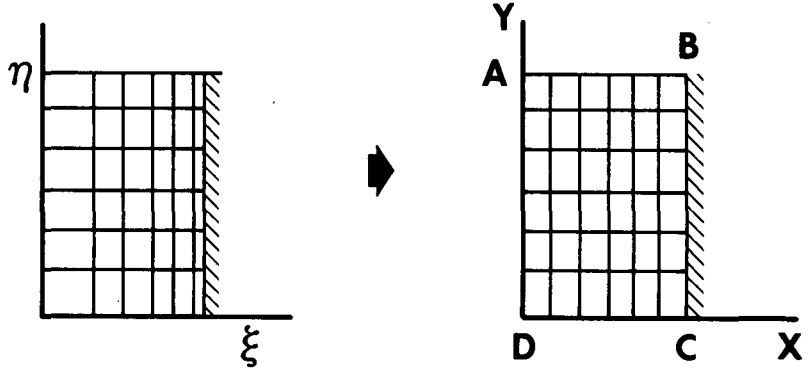

MAPPING 2

Figure 6

EFFECT OF MESH CONSTRUCTION

(Figure 7)

A computer code was written to carry out computations of a viscous flow in the nose region of a hyperboloid with a 10° asymptotic half-angle. The free-stream conditions were given by altitude = 75 km, velocity = 6 km/sec . The wall temperature was assigned to 1,000° K. The effects of mesh on the computational results were investigated under the assumption that the viscosity remained constant in the shock layer. Because of the wall temperature gradient, 20 mesh points were used across the layer and 11 points along the other direction. Convergent or time-asymptotic solutions were found after 500 time steps using 16 minutes on the UNIVAC 1108 system. Oscillations of the temperature profile were observed near the body when the second mapping was not used. The oscillation was damped out for $\beta = 1$ or 2 , where β indicates the degree of squeezing the mesh points toward the cooled body surface. This suggests that the time-dependent technique may provide useful results without resorting to a large number of mesh points in the flow regime close to the thin boundary layer.

EFFECT OF MESH CONSTRUCTION

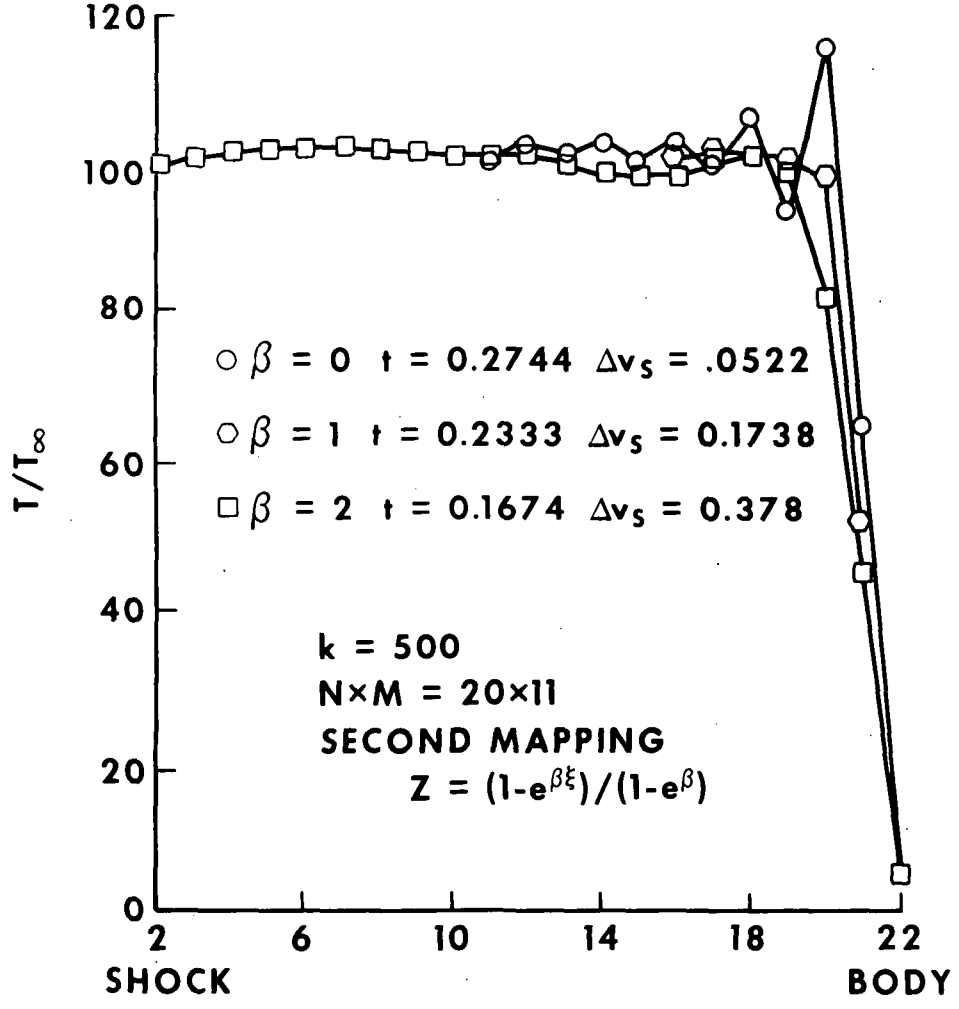

Figure 7

SHOCK SHAPES

(Figure 8)

A series of calculations was made for $Re_\infty = 10^5$, 5000, 500, and 50 to learn the effect of the Reynolds number on the flow field. The results indicated that as the Reynolds number was increased, the shock layer became thinner, and the computation converged to a steady state more rapidly. The steadiness of the solution may be indicated by the value of Δv_s, the range of the shock speed. The noticeably thinner shock layer at the lower Reynolds numbers is because the wall temperature is more strongly diffused upstream, which in turn increases the density inside the layer. Note that the shock shapes in this figure are the inner edges of the shock waves. A separate analysis would be required to obtain the shock wave structure. All calculations except $Re_\infty = 50$ used 500 time steps. The convergence was very slow at lower Reynolds numbers. Solutions generated for $Re_\infty = 50$ required approximately twice the number of time steps to achieve a similar convergent solution for $Re_\infty = 10^5$. Also shown in the same figure is an inviscid solution using velocity slip conditions. The shock wave is very thin and is located closer to the body than the results of $Re_\infty = 5000$ and above. The absence of the boundary layer in the inviscid calculation may have contributed to this result.

SHOCK SHAPES

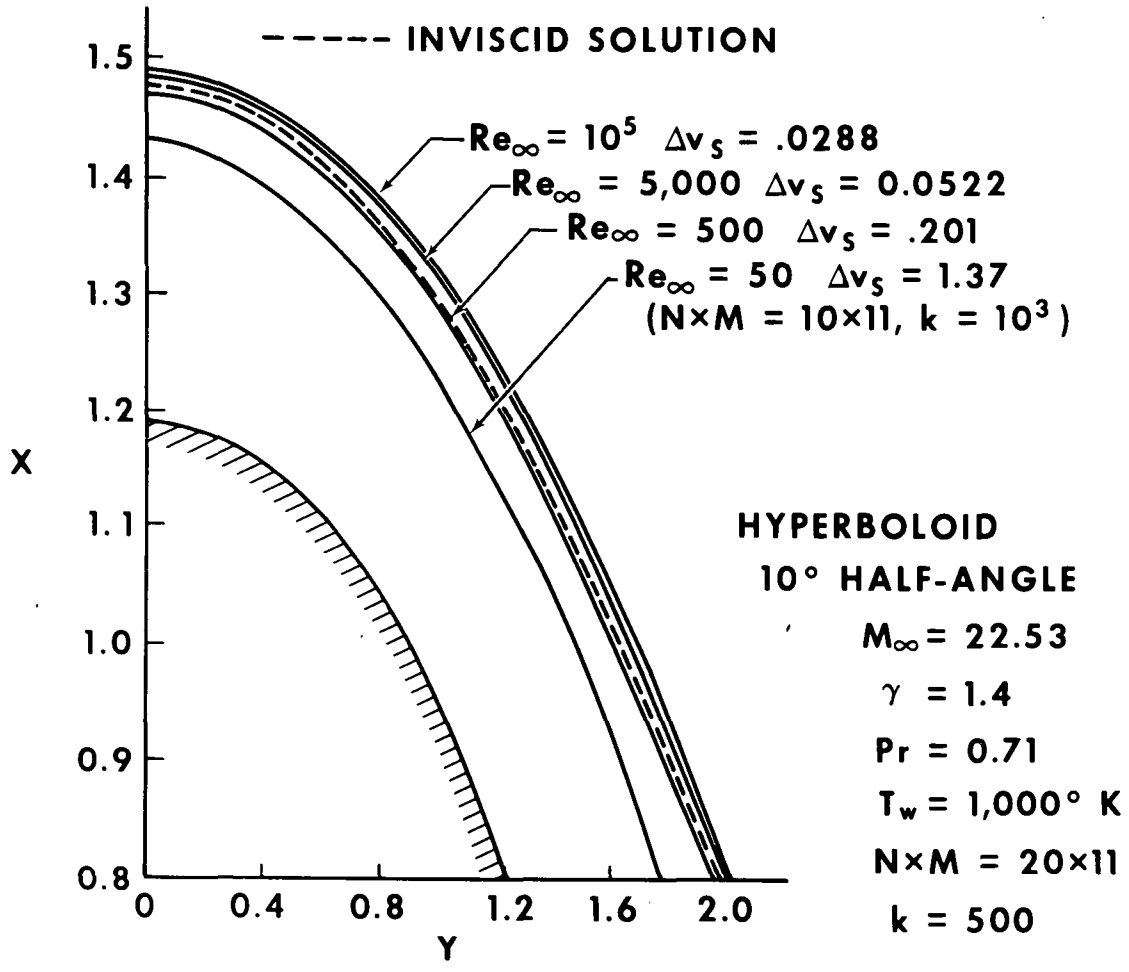

Figure 8

ENTROPY LAYER

(Figures 9(a) and 9(b))

The entropy layer structures are appreciably affected by the Reynolds number. The entropy value is nearly constant along the axis of symmetry for $Re_\infty \geq 500$ but shows an abrupt decrease at the stagnation point and continues decreasing downstream. The nonadiabatic body may be largely responsible for this. The entropy profile at $Re_\infty = 50$ is quite different from the other curves. Its behavior is caused by the merged shock wave and the boundary layer.

The entropy profile obtained for different wall temperatures is also compared with one from an adiabatic condition. The most interesting thing found is that the rate of convergence does not seem to be influenced by the wall temperature.

SURFACE ENTROPY

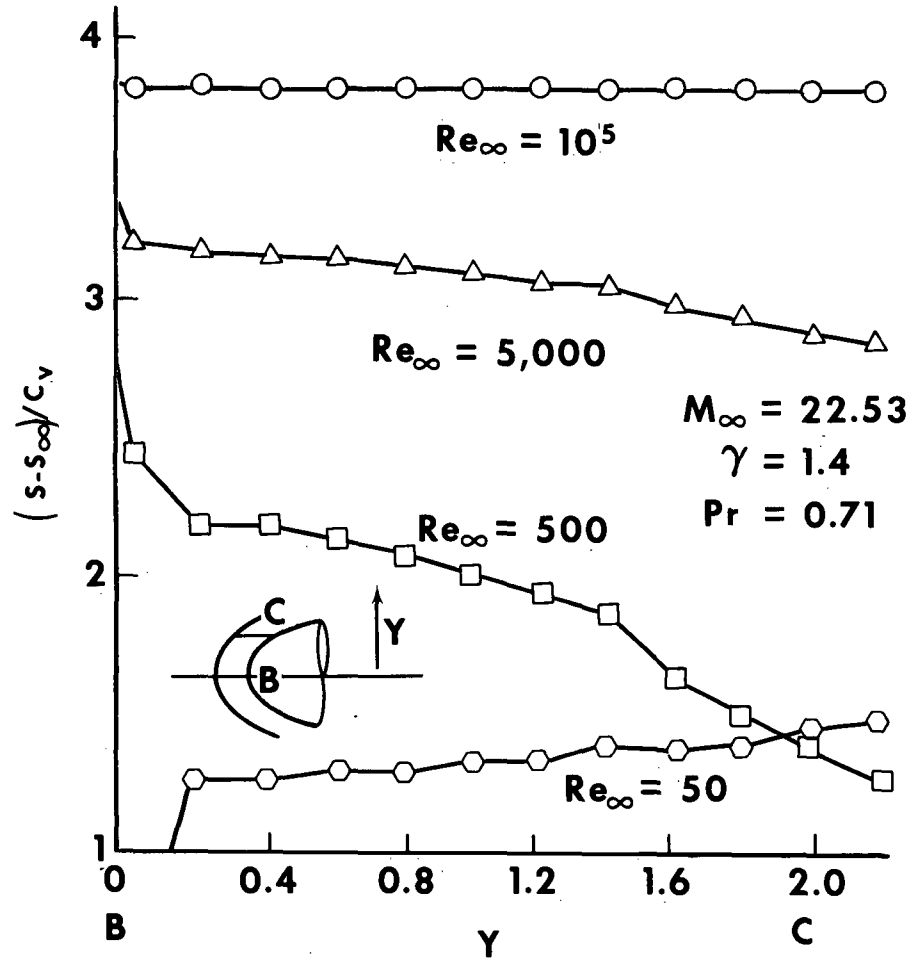

Figure 9(a)

Page intentionally left blank

SURFACE ENTROPY

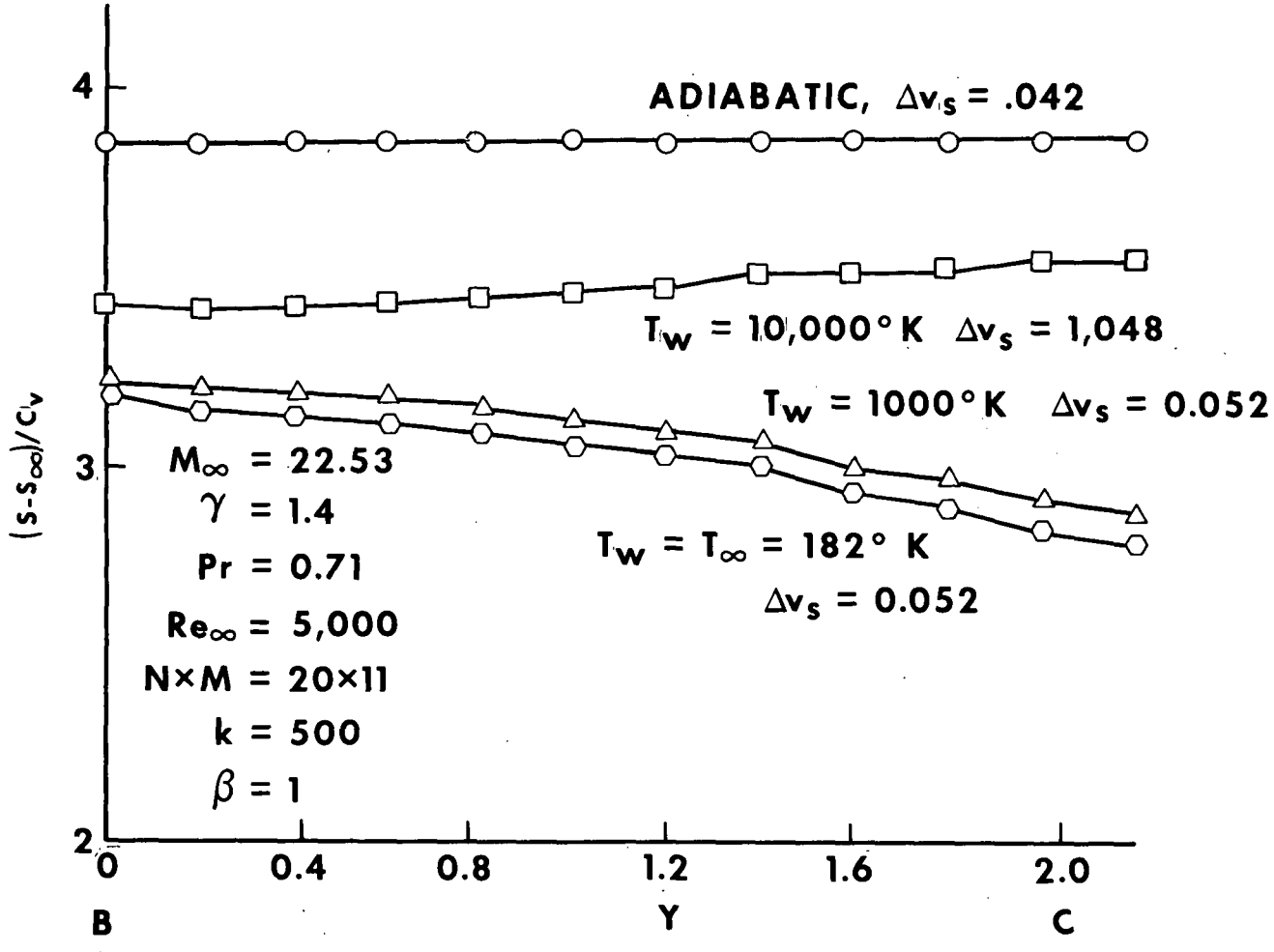

Figure 9(b)

COMPARISON WITH EXPERIMENT AND OTHER THEORIES

(Figure 10)

Experiments to determine heat transfer and skin friction coefficients for blunt-body flows in the regimes other than the thin boundary layer are difficult and scarce. A recent test by Little[7] has raised some question concerning the accuracy of the steady techniques used in predicting the skin friction coefficients C_F close to the stagnation point. Our computed values differ from those of other theories by nearly an order of magnitude; however, they agree very well with the experimental data being extrapolated to the stagnation point. The heat flux coefficient C_H obtained at $Re_\infty = 5000$, however, is quite close to the current theory. Several other results presented in the figure are not compared with either experiments or other theories. Our computed results obtained with 20 mesh points across the shock layer cannot be viewed as highly accurate for flows in the boundary layer regime. Moreover, the results available from other sources have provided too few details in the nose region to warrant a meaningful comparison with our results. The accuracy of the present formulation cannot be judged conclusively at this time.

COMPARISON WITH EXPERIMENT AND OTHER THEORIES

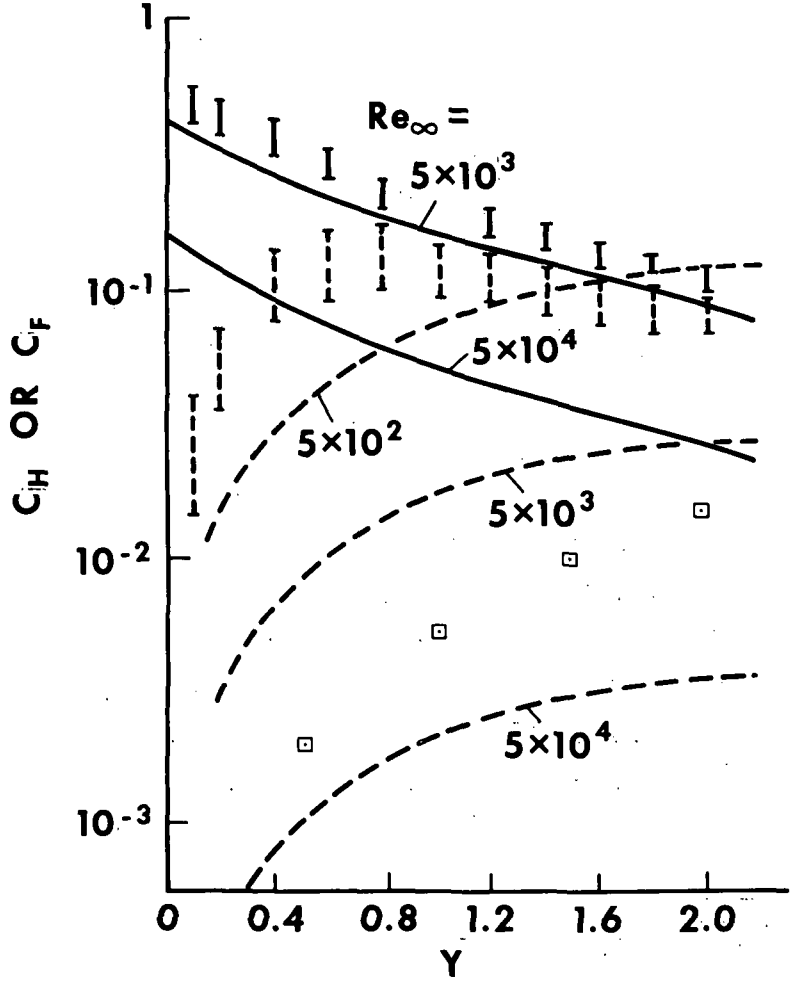

□ C_F FROM EXPERIMENT, $Re_\infty = 2.6\times10^4$

C_F C_H FROM STEADY TECHNIQUES, $Re_\infty = 5.2\times10^3$

---- C_F FROM UNSTEADY TECHNIQUE

—— C_H

$M_\infty = 22$

$h = 75$ KM

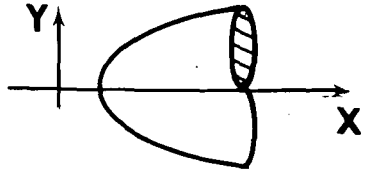

HYPERBOLOID -10°

Figure 10

STARTER SOLUTION IN PROGRESS

(Figure 11)

With the encouraging results obtained from this solution of the full Navier-Stokes equation, a more general and sophisticated formulation is being developed that considers the nonequilibrium phenomena neglected in the present viscous flow study. Both finite-rate chemical reactions and a vibrational harmonic-oscillator model for the diatomic species will be included for a real airflow field calculation. The nonequilibrium phenomena could be significant for the reusable shuttle vehicle. This is particularly true for regions where the surface catalycity affects the surface heat fluxes. This formulation uses the conservative form of the flow equations written on a curvilinear coordinate system. It may economically extend the computational domain further downstream from the subsonic nose region than is allowed by the present Cartesian coordinate system and provide more accurate skin friction and heat flux coefficients at the body surface.

STARTER SOLUTION IN PROGRESS

- CONSERVATIVE-TYPE EQUATIONS
- CURVILINEAR COORDINATE SYSTEM
- FINITE-RATE CHEMICAL REACTION
- HARMONIC-OSCILLATOR MODEL FOR DIATOMIC SPECIES
- CHAPMAN-COWLING 1st APPROXIMATION TO THE TRANSPORT PROPERTY

Figure 11

REFERENCES

1. Kutler, P.; Rakich, J. V.; and Mateer, G. G.: Application of Shock Capturing and Characteristics Methods to Shuttle Flow Fields. Space Shuttle Aerothermodynamics Technology Conference, Vol. I, 1972, pp. 65-92.

2. Probstein, R. F.: Shock Wave and Flow Field Development in Hypersonic Re-entry. ARS Journal, 31, pp. 185-194, February 1961.

3. Cheng, H. K.: Viscous Hypersonic Blunt-Body Problems and the Newtonian Theory in the "Fundamental Phenomena in Hypersonic Flow." Hall, J. G., ed., Cornell University Press, N. Y., pp. 90-132, 1966.

4. Scala, S. M., and Gordon, P.: Solution of the Time-Dependent Navier-Stokes Equations for the Flow Around a Circular Cylinder. AIAA Journal, 6, pp. 815-822, May 1968.

5. Moretti, G., and Abbett, M.: A Time-Dependent Computational Method for Blunt Body Flows. AIAA Journal, 4, pp. 776-782, December 1966.

6. Li, C. P.: Numerical Solutions of the Navier-Stokes Equations for the Shock Layer. TR 675-44-459, Lockheed Electronics Company, Inc., Houston Aerospace Systems Division, August 1971.

7. Little, H. R.: Surface Conditions on Hyperboloids and Paraboloids in Hypersonic Flow. AIAA paper no. 70-182, January 1970.